POLITECNICO DI TORINO
Repository ISTITUZIONALE

Cost Effective 3D Printed Heatsink for Fast Prototyping of WBG Power Converters

Original
Cost Effective 3D Printed Heatsink for Fast Prototyping of WBG Power Converters / Stella, F., Savio, S., Vico, E., Bojoi, R., Armando, E.. - ELETTRONICO. - (2024), pp. 2562-2567. (2024 IEEE Applied Power Electronics Conference and Exposition (APEC) Long Beach, CA, USA 25-29 Febbraio 2024) [10.1109/apec48139.2024.10509035].

Availability:
This version is available at: 11583/2988945 since: 2024-05-23T09:38:53Z

Publisher:
IEEE

Published
DOI:10.1109/apec48139.2024.10509035

Terms of use:

This article is made available under terms and conditions as specified in the corresponding bibliographic description in the repository

Publisher copyright
IEEE postprint/Author's Accepted Manuscript

©2024 IEEE. Personal use of this material is permitted. Permission from IEEE must be obtained for all other uses, in any current or future media, including reprinting/republishing this material for advertising or promotional purposes, creating new collecting works, for resale or lists, or reuse of any copyrighted component of this work in other works.

(Article begins on next page)

05 November 2026

Cost Effective 3D Printed Heatsink for Fast Prototyping of WBG Power Converters

Fausto Stella
DENERG Dipartimento di Energia
Politecnico di Torino
Torino, 10129, Italy
fausto.stella@polito.it

Stefano Savio
DENERG Dipartimento di Energia
Politecnico di Torino
Torino, 10129, Italy
stefano.savio@polito.it

Enrico Vico
DENERG Dipartimento di Energia
Politecnico di Torino
Torino, 10129, Italy
enrico.vico@polito.it

Radu Bojoi
DENERG Dipartimento di Energia
Politecnico di Torino
Torino, 10129, Italy
radu.bojoi@polito.it

Eric Armando
DENERG Dipartimento di Energia
Politecnico di Torino
Torino, 10129, Italy
eric.armando@polito.it

***Abstract*— Power density has become a critical figure of merit in power conversion systems, especially in automotive and aerospace applications. Nowadays, wide band gap (WBG) devices are revolutionizing power conversion by enabling unprecedented levels of efficiency and power density. High power density is possible only with advanced integrated cooling solutions based on custom-made heatsinks that must be properly tailored to match the packages of the WBG devices selected for the application. However, the design and prototyping of custom-made heatsinks, typically crafted from aluminium, require significant cost and time during the converter iterative prototyping phases. To address these challenges, this digest proposes a liquid-cooled heatsink made of a combination of 3D-printed plastic material and aluminium. The proposed heatsink, tailored for rapid prototyping, leads to a drastic reduction in costs and development time compared to traditional aluminium heatsinks. Moreover, the incorporation of plastic material delivers additional benefits, including reduced weight and seamless integration with electronic components, owing to its inherent insulating properties.**

Keywords*— *Rapid Prototyping, Advanced Cooling, Liquid Cooling, Heatsink, 3D Printing, Wide Bandgap.

I. Introduction

The introduction of new families of semiconductors such as WBG devices, based on gallium nitride (GaN) or silicon carbide (SiC) materials has pushed the boundaries of power conversion to unprecedented levels of efficiency and power density [1]-[5]. In sectors such as automotive, aerospace, and military applications, where efficiency and power density are major figures of merit, highly integrated WBG-based converters are now a preferred choice. In this context, it is of paramount importance to provide highly efficient and highly integrated cooling solutions enabling to fully exploit the capabilities of WBG devices. Numerous cooling solutions can be found in existing literature, but the primary aim of this paper is to propose an efficient cooling solution specifically designed for power converter prototyping [6]-[12].

For many industrial applications, where the converter design is highly influenced by cost limitations and the power density is not a primary concern, air-cooling solutions are often preferred due to their lower cost, and easiness of implementation [10]. Nevertheless, in the case of highly integrated power converters requiring high power density, air cooling solutions may not be a viable solution for the product and also for the prototyping phase.

Although bulky off-the-shelf liquid-based heatsinks can be used, they may not be always compatible with the precise form factor and layout of the power converter, especially when discrete power devices are employed. Conversely, a custom cooling design allows integrating the heatsink seamlessly into the converter's structure, optimizing space utilization and enhancing the thermal contact with the heat-generating components. Moreover, implementing a cooling system that approaches the final configuration provides a significant advantage in accurately evaluating the converter's overall performance. However, custom cooling solutions are expensive and may increase the time required by the converter prototyping since multiple designs are usually tested before reaching a final solution [15].

Therefore, the goal of this work is to propose an innovative and cost-effective cooling solution for fast prototyping of power converters. A reduced-size metal

heatsink, tailored for the heat extraction region, is combined with a 3D-printed plastic case designed as an enclosure for the liquid coolant. This hybrid approach allows to achieve a proper balance between cost, performance, and easiness of implementation during the prototyping phase. The metal heatsink ensures efficient heat extraction, while the 3D-printed plastic case offers a flexible and customizable enclosure for the liquid coolant, as well as drastic weight reduction and seamless integration with the power devices. This combination allows for a more accurate representation of the final cooling solution without incurring excessive costs or delays associated with full custom designs. This paper is organized as follows. In Section II a bi-component heatsink consisting of aluminium and ABS material is presented. In Section III finite elements simulations are conducted to evaluate the performance of the proposed solution. In Section IV the proposed solution is compared with alternative solutions including a commercial off-the-shelf heatsink. Different performance indicators are compared. In Section V the bi-component heatsink is experimentally tested with a GaN converter and the finite elements simulations are validated. Finally, in Section VI the presented work is summarized, and suggestions for future improvements are provided.

II. Proposed Bi-Component 3D Printed Heatsink

The overview of the proof of concept heatsink made of aluminium and 3D printed ABS plastic is shown in Fig. 1a. It consists of two identical off-the-shelf thin pin aluminium heatsinks (i.e. Fisher ICK S 32x32x10 mm), originally designed to be used as air-cooling heatsinks for processors. In this case, the aluminium heatsinks are used as heating extraction elements to be placed in direct contact with the heating element (e.g. the case of the power device). These aluminium heatsinks are then placed in a 3D-printed plastic case, which serves the dual purpose of directing the flow of liquid over the surface of the aluminium elements and providing mechanical support to the entire assembly. A 3D CAD of the proposed liquid heatsink showing the liquid flow is reported in Fig. 1b. The two metal heatsinks are firmly mounted on the plastic case using HBM X2 heavy duty bi-component glue, which also acts as a sealant.

A two-level inverter leg (shown in Fig. 1c) using GaN HEMT V08TC65S1A2 (VisIC Technologies), was selected as use case. In particular, the proposed bi-component heatsink has been designed to replace an existing air-cooled heatsink, therefore the mounting holes must be compatible with the ones of the original heatsink.

Therefore, four M4 mounting holes are used to mount the heatsink on the PCB. The shape of the 3D-printed plastic case can be adjusted to meet the geometry and space constraints of the target application while providing optimal liquid flow on the surface of the heating extraction elements. A slot at the top of the heatsink was carved to accommodate the DC link capacitors, as shown in Fig. 1c. The main addressed technical challenges are: the mechanical resistance required to withstand the pressure of the liquid, the water impermeability of the printed plastic, and avoiding the thermal deformation of the plastic. With reference to Fig. 1c, the aluminium heat extraction surface is intentionally larger than the actual surface of the device to be cooled. This prevents high temperatures at the edges of the aluminium elements in direct contact with the ABS case, thus avoiding the risk of melting down the case.

III. Heatsink Thermal Analysis Via FEA Simulation

To evaluate the performance of the proposed solution and to compare it with alternative cooling solutions, FEA (Finite Elements Analysis) simulations have been performed using SolidWorks. Fig. 2 shows the temperature distribution across the custom heatsink, considering the following test conditions: fluid flow rate 5 l/min, inlet fluid temperature 30°C, and ambient temperature 30°C. The boundaries of the two aluminium heatsinks are highlighted by a red dashed line while the boundaries of the two chips are highlighted by a black dashed line. The GaN HEMTs package exhibits a top metallic surface that is interfaced with the metallic heatsinks through two high-performing thermal conductive pads (Tflex HP34 having a thermal conductivity of 34 W/mK). During the FEA simulation, the thermal pads have been neglected and the chip surface has been placed in direct contact with the metallic heatsink.

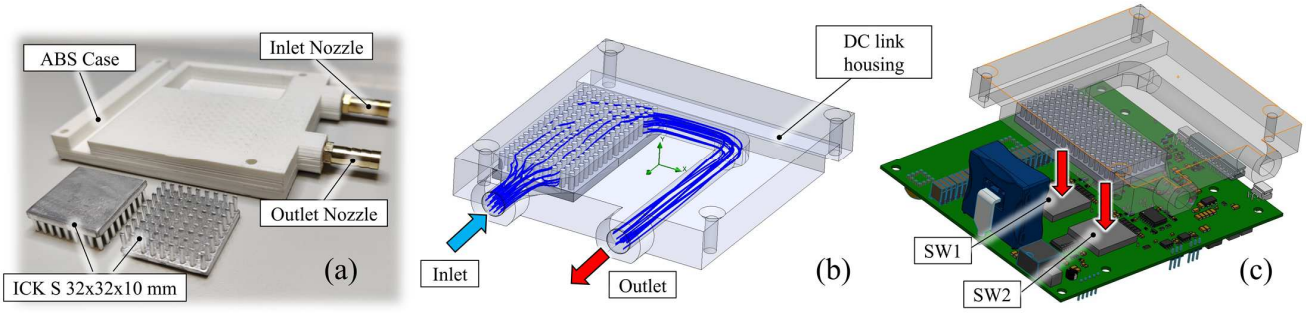


Fig. 1. Proposed heatsink solution consisting of two metal heatsinks enclosed in an ABS 3D case. a) Overview of the realized prototype b) 3D model of the heatsink showing the liquid flow. c) Target application: two-level inverter leg (SW1 and SW2 are GaN 650V/200A V08TC65S1A2 from VisIC).

A dissipated power of 200W is assumed on the surface of each GaN HEMT package, as this scenario represents the worst-case operating condition for the target converter. By looking at the temperature distribution on the metallic heatsink surface it is possible to note that a maximum hotspot temperature of 56°C is reached at the centre of the packages, while the temperature gradually decreases as it approaches the metallic heatsink boundaries. The highest temperature reached at the border of the metallic heatsink (i.e. contact area with the plastic case) is 47.7°C. This value must be carefully checked to ensure to not overcome the HDT (Heat Deflection Temperature) of the plastic material, over which the material loses its mechanical properties and starts to warp. In this case, the compound of ABS material used during the tests starts losing its mechanical properties around 60°C. It is however possible to select material with much higher HDT as later explained.

The calculated average temperature on the surface between the two aluminium heatsinks and the plastic case is approximately 40°C. This value serves as an indicator of the performance of the proposed heatsink when compared to a fully aluminium counterpart (i.e., where the plastic case is replaced with aluminium). Specifically, if the temperature at the heatsink boundary approaches that of the coolant, it signifies that augmenting the metallic material surrounding the chip would not yield any performance enhancements in heat extraction. By looking at Fig. 2, it is also possible to note the presence of 45-degree grooves between the metallic heatsink and the plastic case. These have been added only to accommodate the sealant glue. The sealant glue between the metallic elements and the plastic case has not been considered as the heat transfer between the metallic elements and the plastic case is minimal therefore the precise thermal modelling of the glue would not impact significantly on the results.

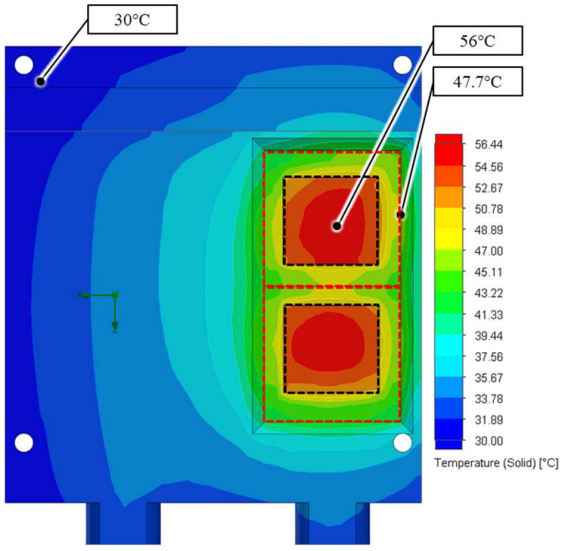


Fig. 2. FEA simulation result of the custom heatsink, showing the significant isotherm temperature contours. The aluminium heatsink boundaries are highlighted by a red dashed line, while the chip boundaries are highlighted with a black dashed line.

IV. Heatsink Performance Comparison

To evaluate the performance of the proposed solution against possible alternatives, FEA simulations have been performed in SolidWorks for the proposed solution and a commercial heatsink. CP4A-114A-108E), as shown in Fig. 3.

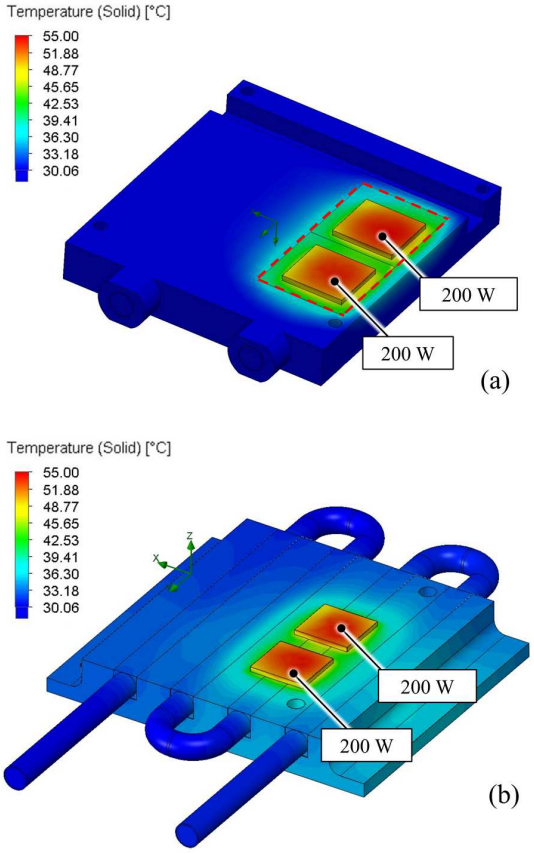


Fig. 3. FEA simulation result. a) Bi-component heatsink. The contact area between the metallic heatsink and the case is highlighted by a red dashed line. b) Commercial CP4A-114A-108E heatsink.

Four cooling solutions are compared: 1) Bi-component heatsink made of aluminium and ABS (i.e. same as the proposed solution), 2) Bi-component heatsink identical to case 1 but with the aluminium material replaced by copper. 3) same as 1 but ABS is replaced with aluminium (i.e. fully custom aluminium case). 4) commercial off-the-shelf heatsink (i.e. CP4A-114A-108E).

The same test conditions of the previous section are considered: fluid flow rate 5 l/min, inlet fluid temperature 30°C, ambient temperature 30°C, power dissipated per power device 200 W. The comparison results are summarized in Table I, where four performance indicators are compared: (1) the thermal resistance $R_{th(case-liquid)}$ between the package case to fluid, (2) the maximum temperature reached in the contact area between the metal elements and the plastic material case (dashed red line in Fig. 3a), (3) the total weight, and (4) the pressure drop between the inlet and the outlet of the heatsink. The $R_{th(case-liquid)}$ has been computed as [16]:

$$R_{th(case-liquid)} = \frac{T_{\text{case}} - T_{\text{liquid}}}{P} \quad (1)$$

The thermal resistance package surface to fluid of the ABS-aluminium solution computed with (1) is 0.103°C/W for SW1 and 0.101°C/W for SW2. These values closely resemble those obtained when utilizing a commercial heatsink, such as the CP4A-114A-108E, with a negligible difference of approximately 5% in thermal resistance. Furthermore, the proposed heatsink is compared with a fully aluminium one, where the same geometry is maintained but the ABS material is replaced by aluminium. In this case, the results show that replacing the plastic material with aluminium enables achieving only a marginal reduction of the thermal resistance.

A possible alternative of the proposed solution is to replace the aluminium heatsinks with other heatsinks made of material with better thermal conductivity. In this case, the thermal resistance is considerably lower compared to all the other solutions. This remarkable outcome underscores that by utilizing a lower resistivity material for the heat extraction elements, such as copper, it is possible to achieve even better performance than with a fully metallic heatsink made of a higher conduction resistance material, such as aluminium. While a full copper heatsink might be prohibitively expensive for many practical applications, a hybrid heatsink consisting of copper and ABS is likely to be more cost-effective and better performing than a fully aluminium one. The maximum temperature at the border between the metal heatsink and the plastic case is reported in Table I, in the case of heating extraction elements made of aluminium or copper. In this latter case, the maximum temperature at the border of the metallic elements is lower due to the better conductivity of the chopper which helps the heating transfer between the chips surfaces and the liquid. If this interface temperature becomes critical for the plastic material, it is possible to increase the area of the heating extraction element or alternatively, it is possible to replace the plastic material with one with a higher HDT.

Although the weight may not be critical during the prototyping stage, it can become a major figure of merit if the proposed solution is further industrialized and used in applications such as automotive or aerospace. The proposed solution is 2.3 times lighter compared to a fully aluminium equivalent solution and 4.6 lighter compared to the commercial solution. Pressure drop is also reported as an indicator, however, the material of the heatsink does not impact significantly on it. This value can be adjusted by varying the geometry of the heatsink. Other indicators such as the mechanical roughness of the material are not considered. However, these considerations will be crucial in the event of further industrialization of the proposed solution, which will include the optimal selection of plastic material, sealant glue, and geometry.

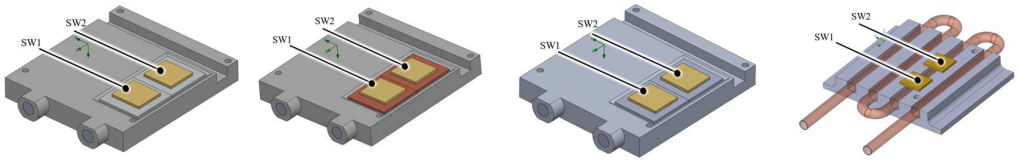
Another noteworthy aspect to consider is the electrical conductivity of the heatsink. In the case of hybrid solutions, the plastic component can be considered as an insulator, thus allowing it to be placed in direct contact with live parts of the converter. This can be considered a significant point of merit in high-power density applications. Additionally, the 3D printing of plastic components enables the creation of complex geometries without the necessity for complex and costly mechanical processing.

V. Experimental Validation

The proposed heatsink was mounted and tested on the target converter, as shown in Fig.4, while its temperature was monitored using four thermistors, thus validating the FEA simulation and assessing the mechanical resistance. The heatsink was tested for 3 hours at a pressure of 3 bar while the total loss on the two GaN devices was 300 W and no deformations have been observed.

Table I: Performance Comparison for Different Heatsinks Solutions

Properties	ABS-Aluminium	ABS-Copper	Full Aluminium	Commercial
$R_{th,case-liquid,SW1}$ [°C/W]	0.103	0.078	0.098	0.107
$R_{th,case-liquid,SW2}$ [°C/W]	0.101	0.075	0.095	0.107
$T_{max,boder}$[°C]	47.68	44.02	//	//
$Weight[g]$	164	231	378	766
$Pressure\ Drop$[°C]	7046	7046	7046	3956



The initial version of the heatsink was 3D printed using a low-cost 3D printer with limited performance capabilities. After extended usage, a minor water exudation was noticed within the plastic due to the presence of micro holes between the plastic filaments. To address this issue, a waterproofing paint was applied to cover the external surface of the heatsink. Later, a second heatsink was produced using a higher-grade 3D printer, and in this case, no water exudation was observed.



Fig. 4. Bi-component heatsink mounted on the target GaN inverter leg.

VI. Conclusions

A bi-component heatsink consisting of 3D-printed plastic material and metal has been proposed in this paper. The main benefits are the reduced cost and manufacturing time, thanks to the widespread availability of 3D printers for plastic materials. Although this bi-component heatsink was proposed for rapid prototyping, it is very promising also for commercial products using discrete WBG devices, offering significant advantages in terms of cost reduction and weight savings.

The thermal performance, assessed through FEA simulations and experimental validation, has shown that the ABS-Aluminium solution provides thermal characteristics comparable to those of full-size commercial heatsinks. For simplicity reasons, off-the-shelf aluminium parts have been used, however, custom heating extraction elements using copper can be designed to further improve the performance of the proposed solution at a reasonable cost. Furthermore, the 3D-printed plastic case can be meticulously designed to align with the specific needs and spatial constraints of the converter system, thus facilitating seamless integration and optimizing heat dissipation.

For this prototype, ABS was selected as the plastic material. However, other plastic materials with higher meltdown temperatures can be used, such as the material presented in [17] with HDT (0.45 MPa ,238°C), thus enabling to operate with higher liquid temperatures.

An additional benefit of the proposed solution is the insulating properties of the plastic material that can be put in contact with live parts. For example, power components of the converter such as busbars can be integrated into the plastic material of the DC link without the need for additional insulation.

Applications that would most benefit from the proposed solution are the ones with a “complex” power layout, where multiple power switches are used such as onboard chargers [18] and [19], multi-level converters, multi-phase machine converters, matrix converters [20] and so on.

Acknowledgements

This study was carried out within the MOST – Sustainable Mobility Center and received funding from the European Union Next-GenerationEU (PIANO NAZIONALE DI RIPRESA E RESILIENZA (PNRR) – MISSIONE 4 COMPONENTE 2, INVESTIMENTO 1.4 – D.D. 1033 17/06/2022, CN00000023). This manuscript reflects only the authors’ views and opinions, neither the European Union nor the European Commission can be considered responsible for them.

References

[1] L. Zhang, X. Yuan, X. Wu, C. Shi, J. Zhang, and Y. Zhang, “Performance Evaluation of High-Power SiC MOSFET Modules in Comparison to Si IGBT Modules,” IEEE Transactions on Power Electronics, vol. 34, no. 2, pp. 1181–1196, Feb. 2019.

[2] F. Stella, E. Vico, D. Cittanti, C. Liu, J. Shen, and R. Bojoi, “Design and Testing of an Automotive Compliant 800V 550 kVA SiC Traction Inverter with Full-Ceramic DC-Link and EMI Filter,” in 2022 IEEE Energy Conversion Congress and Exposition (ECCE), Oct. 2022.

[3] D. Cittanti et al., “Analysis and Design of a High Power Density Full-Ceramic 900 V DC-Link Capacitor for a 550 kVA Electric Vehicle Drive Inverter,” in 2022 International Power Electronics Conference (IPEC-Himeji 2022- ECCE Asia), May 2022, pp. 1144–1151. doi: 10.23919/IPEC-Himeji2022-ECCE53331.2022.9807220.

[4] F. Mandrile et al., “Grid Fault Current Injection Using Virtual Synchronous Machines Featuring Active Junction Temperature Limitation of Power Devices,” IEEE Journal of Emerging and Selected Topics in Power Electronics, vol. 10, no. 5, pp. 6243–6251, Oct. 2022, doi: 10.1109/JESTPE.2022.3154488.

[5] F. Stella, G. Pellegrino, E. Armando, and D. Daprà, “Advanced testing of SiC power MOSFET modules for electric motor drives,” in 2017 IEEE International Electric Machines and Drives Conference (IEMDC), May 2017, pp. 1–8. doi: 10.1109/IEMDC.2017.8002314.

[6] E. Laloya, Ó. Lucía, H. Sarnago and J. M. Burdío, "Heat Management in Power Converters: From State of the Art to Future Ultrahigh Efficiency Systems," in IEEE Transactions on Power Electronics, vol. 31, no. 11, pp. 7896-7908, Nov. 2016, doi: 10.1109/TPEL.2015.2513433.

[7] K. Deepak, M. -T. Tran, D. -D. Tran, M. El Baghdadi and O. Hegazy, ”Design Investigation of Liquid Cooled Heat Sink for GaN FET Dual-Three Phase Inverter,” 2022 International Symposium on Power Electronics, Electrical Drives, Automation and Motion (SPEEDAM), Sorrento, Italy, 2022, pp. 149-154.

[8] B. Agostini, M. Fabbri, J. E. Park, L. Wojtan, J. R. Thome, e B. Michel, ”State of the Art of High Heat Flux Cooling Technologies”, Heat Transfer Engineering, vol. 28, fasc. 4, pp. 258–281, apr. 2007

[9] S. N. Joshi et al., ”A Review of Select Patented Technologies for Cooling of High Heat Flux Power Semiconductor Devices,” in IEEE Transactions on Power Electronics, vol. 38, no. 6, pp. 6790-6794, June 2023.

[10] D. Sabatino and K. Yoder, "Pyrolytic Graphite Heat Sinks: A Study of Circuit Board Applications," in IEEE Transactions on Components, Packaging and Manufacturing Technology, vol. 4, no. 6, pp. 999-1009, June 2014, doi: 10.1109/TCPMT.2014.2314618.

[11] M. B. Dogruoz and M. Arik, "An investigation on the conduction and convection heat transfer from advanced heat sinks," 2008 11th Intersociety Conference on Thermal and Thermomechanical Phenomena in Electronic Systems, Orlando, FL, USA, 2008, pp. 367-373, doi: 10.1109/ITHERM.2008.4544293.

[12] P. Ning, F. Wang and K. D. T. Ngo, ”Forced-Air Cooling System Design Under Weight Constraint for High-Temperature SiC Converter,” in IEEE Transactions on Power Electronics, vol. 29, no. 4, pp. 1998-2007, April 2014.

[13] Ki Wook Jung, Chirag R. Kharangate, Hyoungsoon Lee, James Palko, Feng Zhou, Mehdi Asheghi, Ercan M. Dede, Kenneth E. Goodson,

Embedded cooling with 3D manifold for vehicle power electronics application: Single-phase thermal-fluid performance, International Journal of Heat and Mass Transfer, Volume 130, 2019, Pages 1108-1119.

[14] T. Wu, B. Ozpineci, M. Chinthavali, Zhiqiang Wang, S. Debnath and S. Campbell, "Design and optimization of 3D printed air-cooled heat sinks based on genetic algorithms," 2017 IEEE Transportation Electrification Conference and Expo (ITEC), Chicago, IL, 2017, pp. 650-655, doi: 10.1109/ITEC.2017.7993346.

[15] P. S. Niklaus, J. W. Kolar, e D. Bortis, "100 kHz Large-Signal Bandwidth GaN-Based 10 kVA Class-D Power Amplifier With 4.8 MHz Switching Frequency", IEEE Trans. Power Electron., vol. 38, fasc. 2, pp. 2307–2326, feb. 2023.

[16] Semikron application note AN1404 Revision 01 Issue date: 2014-11-30: "Thermal resistance of IGBT Modules-specification and modelling". URL: https://www.semikron.com/dl/service-support/downloads/download/semikron-application-note-thermal-resistances-of-igbt-modules-en-2014-11-30-rev-01/

[17] High-temperature resin. URL: https://www.weerg.com/3d-printing-materials/resin/high-temperature-resin

[18] M. Martino, P. Pescetto and G. Pellegrino, "Advanced Functionally Integrated E-Axle for A-Segment Electric Vehicles," 2020 AEIT International Conference of Electrical and Electronic Technologies for Automotive (AEIT AUTOMOTIVE), Turin, Italy, 2020, pp. 1-6, doi: 10.23919/AEITAUTOMOTIVE50086.2020.9307382.

[19] M. Valente, T. Wijekoon, F. Freijedo, P. Pescetto, G. Pellegrino and R. Bojoi, "Integrated On-Board EV Battery Chargers: New Perspectives and Challenges for Safety Improvement," 2021 IEEE Workshop on Electrical Machines Design, Control and Diagnosis (WEMDCD), Modena, Italy, 2021, pp. 349-356, doi: 10.1109/WEMDCD51469.2021.9425666.

[20] F. Stella, A. Yousefi-Talouki, S. Odhano, G. Pellegrino, and P. Zanchetta, "An Accurate Self-Commissioning Technique for Matrix Converters Applied to Sensorless Control of Synchronous Reluctance Motor Drives," IEEE Journal of Emerging and Selected Topics in Power Electronics, vol. 7, no. 2, pp. 1342–1351, Jun. 2019, doi: 10.1109/JESTPE.2018.2851142.